Effectiveness of a dynein team in tug-of-war helped by reduced load-sensitivity of detachment: evidence from study of bidirectional endosome transport in *D. discoideum*

Deepak Bhat, Manoj Gopalakrishnan

Department of Physics, Indian Institute of Technology Madras, Chennai 600036, India

E-mail: `manoj@physics.iitm.ac.in,deepak@physics.iitm.ac.in`

Abstract. Bidirectional cargo transport by molecular motors in cells is a complex phenomenon, in which the cargo (usually a vesicle) alternately moves in retrograde and anterograde directions. In this case, teams of oppositely pulling motors (eg., kinesin and dynein) bind to the cargo simultaneously, and 'coordinate' their activity such that the motion consists of spells of positively and negatively directed segments, separated by pauses of varying duration. A set of recent experiments have analyzed the bidirectional motion of endosomes in the amoeba *D. discoideum* in detail. It was found that in between directional switches, a team of 5-6 dyneins stall a cargo against a stronger kinesin in tug of war, which lasts for almost a second. As the mean detachment time of a kinesin under its stall load was also observed to be $\sim$ 1s, we infer that the collective detachment time of the dynein assembly must also be similar. Here, we analyze this inference from a modeling perspective, using experimentally measured single-molecule parameters as inputs. We find that the commonly assumed exponential load-dependent detachment rate is inconsistent with observations, as it predicts that a 5-dynein assembly will detach under its combined stall load in less than a hundredth of a second. A modified model where the load-dependent unbinding rate is assumed to saturate at stall-force level for super-stall loads gives results which are in agreement with experimental data. Our analysis suggests that the load-dependent detachment of a dynein in a team is qualitatively different at sub-stall and super-stall loads, a conclusion which is likely to have implications in other situations involving collective effects of many motors.

1. Introduction:

Active cellular transport is made possible by ATP-consuming motor-proteins, i.e., kinesin, dynein and myosin which walk on the polar cytoskeletal filaments. Kinesin and Dynein are microtubule-associated motors while myosin is actin-based. The directionality of motor motion is derived from the structural polarity of the corresponding filament and the irreversibility of ATP hydrolysis reaction which powers the motion. Dynein is involved in minus directed (towards center of the cell) transport where as, kinesin shows plus (towards periphery of the cell) directed motion on microtubules. Both kinesin and dynein are involved in transport of intracellular vesicles and other cargoes. Many intracellular cargoes are known to move in a bidirectional fashion, where the direction of motion is reversed typically every few seconds (reviewed in [1, 2]). Examples of such cargoes include mitochondria, pigment granules, endosomes and viruses. Bidirectional motion results from competition between oppositely pulling motors, which bind the same cargo. Two mechanisms have been envisaged in this context, both of which can cause bidirectional motion, i.e., (a) *tug of war* and (b) *reciprocal coordination*. In the first case, motors actively pull against each other, leading to tug of war (TOW) situations. When one team wins (by enhancing detachment of the opposite team), it moves the cargo in its direction, until one or more of the other motors bind. In the second case, a pre-existing regulatory protein complex is assumed to mediate the motor-filament interaction, which switches on and switches off the plus and minus-directed motors alternately. Several candidates have been proposed to perform the role of such a complex, eg. Klar and dynactin[2].

Recently, Soppina et al [3] reported a series of in vivo and in vitro experiments with endosomes in the amoeba *Dictyostelium discoideum* (henceforth, simply *Dictyostelium*). The observed endosome motion was bidirectional, and showed three distinct phases, including positively and negatively directed unidirectional motion and a TOW phase where the cargo stalled as a result of being pulled in both directions by motor teams exerting approximately equal force (although a small negatively directed velocity of a few nm/s was observed in this phase, indicating that one motor team was slightly stronger than the other). The endosome was also observed to undergo fission in some of the TOW situations, which suggests a new functional role for the bidirectional transport.

Detailed analysis using optical trapping suggested that an endosome is transported by one kinesin and 5-6 cytoplasmic dyneins. It was determined that the stall force of the kinesin is 5.5 pN, while that for dynein is 1.1 pN, showing that the kinesin is almost 5 times stronger than a single dynein. Furthermore, the motors were found to have very different tenacity: under stall load, it was determined that the kinesin would detach in a time scale of about 1 second. Since the mean duration of the TOW was also close to 1 second, it is necessary that the opposing team of dyneins do not detach faster (as then the TOW would end sooner, and preferentially in favor of kinesin). The mean detachment time of a single dynein under an opposing load equal to its stall force was determined to be only about 0.2 seconds. Therefore, it is important to ensure that,

as the number of dyneins in the team is increased, the mean detachment time under the (combined) stall load (later referred to as the *stall time*) also increases, so that a team of 5-6 dyneins is an effective competitor against a strong, tenacious kinesin. The relationship between the stall time of a motor assembly and the number of motors is far from obvious, though. As we show in a later section, in the context of the present experiments, increase of stall time with motor number requires that the detachment rate, which normally increases under opposing load, saturates (or possibly increases much slower than exponential) at super-stall loads. We will show that this conjecture is consistent with the endosomal bidirectional transport data reported in[3] and the human adenovirus transport data reported in[4].

From a more general perspective, to what extent the properties of a multiple-motor assembly may be deduced from the physical parameters that characterize the individual motors, is a question that merits attention. Recent experimental observations have thrown up many surprises, such as a cargo carried by two motors does not necessarily travel longer on a filament without detachment compared to one motor *in vivo*[5]. Computational modeling of multiple motor systems with built-in interaction between motors has predicted sub-additive stall forces[6]. These results indicate that the different motors working in a team likely interact with each other. However, such interactions are difficult to model directly owing to the complex structure of motor proteins. Therefore, an indirect way to deduce information about motor-motor interactions would be to compare the predictions of simple *in silico* motor models (where direct interactions are deemed absent) with experimental results.

A recent interesting paper by Kunwar et. al.[7] has reported experimental and modeling studies of bidirectional transport of lipid droplets in *Drosophila* embryos. In this work, the authors attempted to fit the experimentally observed parameters of transport, like the mean pause duration, frequency of pauses and the statistics of the unidirectional run lengths to predictions from a tug-of-war model. The authors used both a 'mean-field' TOW model (as in, eg., [8, 9]) where same-polarity motors share opposing load equally, as well as a more sophisticated model where load-sharing is stochastic and uneven[6]. It is reported that neither of these models agree quantitatively with the in vivo experiments, suggesting that further regulatory mechanisms may be in place to regulate the transport. Interestingly, *in vitro* bead experiments also showed that the detachment rate of dynein as a function of opposing force is non-monotonic, with a peak around 2pN and possibly saturating at very high loads (up to 10pN), in disagreement with the commonly used exponential detachment rate. It was also noted that the disagreement with experimental data would be worse if the exponential detachment rate is used, instead of the non-monotonic, experimentally determined curve.

In this paper, we report a detailed analysis of the bidirectional endosome transport data reported in Soppina et. al. The individual single molecule parameters are extracted from in vitro data reported in the same paper. These parameters are then used to simulate the bidirectional endosome transport *in silico*, using the stochastic model first introduced in Müller et. al.[8, 9], which itself is based on the earlier work by Klumpp and

Lipowsky[10]. We show that the the observed pause/TOW durations are inconsistent with an exponential increase in detachment rate with opposing load, for dyneins. A modified detachment rate which saturates above the stall force is found to agree much better with the experimental data, which is consistent with (and arrived independently of) the lipid droplet results presented in [7]. Moreover, similar to Kunwar et. al., we are also unable to reproduce the experimentally observed unidirectional run lengths within our model, suggesting, among other possibilities, the presence of a regulating factor/switch.

In the rest of the paper, we first describe the experimental results of Soppina et. al. in brief. We then explain the salient features of our model, with the assumptions used, analyze the experimental results using the model, discuss our results and present our conclusions.

2. Review of experimental results for endosome transport in Dictyostelium

Several experiments have shown bidirectional motion of cargoes inside living cells, eg., pigment granules[11], lipid droplets[12, 13], endosomes[13, 14] and several types of viruses[15, 16, 17]. However, in most cases, the precise mechanism that regulates the switching between plus and minus end directed motion remains unclear. In contrast, a few experiments[3, 18] have shown direct evidence for TOW between opposing teams of motors. In Soppina et. al.[3], the motion of early endosomes in the amoeba *Dictyostelium* was studied in detail, and parameters characterizing the bidirectional transport are measured. *In vivo* observations showed bidirectional motion of the cargo with frequent 'triphasic' reversals, which occasionally terminated in fission of the endosomes. Reversal in direction was characterized by a slow phase (cargo velocity of a few nm/s) sandwiched between two oppositely directed, fast unidirectional runs (velocity nearly 2.1 μm/s). The mean duration of the slow phase was about 0.8 seconds. Endosomes elongated up to 25% of its length in this slow moving phase which sometimes ended in fission. Forces of 11-18pN are sufficient to produce tubes from membrane of golgi apparatus and endoplasmic reticulum [19]. So, the elongation and fission of endosome is because of high activity of one to two kinesins pulling against five to eight dyneins which can effectively produce tension of 11-18pN.

Soppina et. al. also performed a number of *in vitro* optical trap experiments to complement the *in vivo* observations. Endosome motion was reconstituted in *Dictyostelium* cell extracts, and the motion was very similar to that observed *in vivo*. Individual molecular motor properties were analyzed using optical trap on motor coated plastic beads. Molecular motors purified from *Dictyostelium* cells were bound to the beads and made to move under controlled loads. Single motor run lengths and velocities were measured for both dynein and kinesin. Stall force for one dynein is found to be 1.1pN whereas that for kinesin is 5.5pN. Stall force for two and three dyneins were 2.2pN and 3.3pN respectively. The additive stall force for multiple motors showed equal load sharing by engaged motors. Importantly, the mean duration for which a single motor

Kind of motor	motor number (n)	velocity $v_\pm$ $(\mu m s^{-1})$	runlength $l_\pm$ (μm)	Stall force(F_s) (pN)	Stall time $T_\pm^n(F_\pm^s)$ (s)
Dynein $(-)$	1	1.2	1.8	1.1	0.2± 0.1
	2	1.5	8	2.2	0.4± 0.2
	3	1.5	15	3.3	0.6 ± 0.4
Kinesin $(+)$	1	1.6	5.1	5.5	1.1
	2	1.6	15	11	ND

Table 1. A list of parameters measured from *in vitro* motion of motor-coated plastic beads, as reported in [3].

Type of event	pre-reversal run time(s)	TOW duration(s)	post-reversal run time(s)
plus→ minus	5	0.9	8.69
minus→ plus	8.69	1.1	5

Table 2. The table lists the bidirectional transport parameters obtained from motion of endosomes in *Dictystelium* cell extracts, as reported in [3], Table S1 therein. All times are in seconds. The run times are obtained from run lengths (measured) and velocities (measured to be in the range ~ 2.0-$2.3\mu m/s$). Error bars are omitted from this table.

or a team of motors survive in the trap without detachment against its respective stall force (henceforth referred to as "stall time") was measured using beads coated with varying number of dyneins.

Table 1 summarizes the results from *in vitro* studies. Note that the stall time increases almost linearly with the number of dyneins, and extrapolation to five dyneins would give a stall time of 1s, which matches closely with the observed TOW duration *in vivo*. The endosomes also undergo considerable stretching during the TOW events as discussed previously, and the time-scale of elongation may vary between a fraction of a second to to almost a second (Fig.S2, Supplementary Index of [3]). This time-delay in the transmission of load across the endosome caused by elongation is also likely to be important in determining the TOW duration *in vivo*, but this obviously does not apply to motor-coated beads which show clearly an upward trend in the stall time with the number of engaged motors. Therefore, in this paper, we will focus on cargo-independent motor properties as far as explaining the stall time or TOW duration is concerned.

A summary of important parameters characterizing *in vivo* observations of bidirectional endosome transport is given in Table 2. In the next section, we discuss our mathematical model which is used to analyze these observations.

3. Stochastic model

For quantitative analysis of the data, we use the stochastic model described in Müller et al [8]. In this model, a cargo is assumed to be bound to a certain fixed number of motors of either directionality. The motors are assumed to be always bound to the

cargo, but may attach to and detach from the filament stochastically. The opposing load is assumed to be shared by similar motors equally, which is a simplifying feature of this 'mean-field' model, in which there is no direct motor-cargo or motor-motor interactions. Other models have been proposed which include both motor-cargo[6, 20] and motor-motor[21, 22] interactions in more detail, as a consequence of which load-sharing by motors also becomes stochastic. In this paper, we ignore these effects for the sake of simplicity.

Consider a cargo with D attached dyneins and K attached kinesins moving on a microtubule. The state of the cargo at a given point of time may be denoted by $|dk\rangle$, where $d \leq D$ is the number of dyneins attached to the filament, and $k \leq K$ is the number of kinesins attached to the filament. In the model in [8], the forces exerted by individual motors are determined dynamically through a set of self-consistent equations based on balance of forces on the cargo, and phenomenological equations that describe the decrease in velocity with load. These equations yield the cargo velocity $v_c(d, k)$ and the dynamic load $F_c(d, k)$ as functions of the numbers of filament-engaged motors. While calculating $v_c(d, k)$ and $F_c(d, k)$, a piecewise linear force-velocity relation is assumed for each type of motor:

$$
\begin{aligned}
v_\pm(\lambda_\pm) &= v_\pm \left(1 - \frac{\lambda_\pm}{F_s^\pm} \right) && : \lambda_\pm \leq F_S^\pm \\
&= v'_\pm \left(1 - \frac{\lambda_\pm}{F_s^\pm} \right) && : \lambda_\pm \geq F_S^\pm
\end{aligned}
\tag{1}
$$

where $v_\pm$ and $v'_\pm$ are absolute values of motor forward and backward velocities, while $\lambda_\pm$ denote the load per motor (under the assumption of equal load sharing), given by

$$
\lambda_+ = \frac{F_c(d, k)}{k} \quad ; \quad \lambda_- = \frac{F_c(d, k)}{d}
\tag{2}
$$

For the sake of consistency in the model, a non-zero absolute backward velocity $v'_\pm$ is considered for both the motors with values $v'_+ = 6$ nm s^{-1} for kinesin and $v'_- = 72$nm s^{-1} for dynein [8]. Forward velocity of a kinesin and a dynein respectively taken as $v_+ = 1.6\mu$m s^{-1} and $v_- = 1.2\mu$m s^{-1} from in-vitro studies reported in [3](see Table 2). We would like to emphasize that the precise form of the force-velocity curve and the absolute values of of the backward velocities are not crucial ingredients for the model.

Let $\epsilon_+(d, k)$ and π_+ denote the detachment and attachment rate of an individual kinesin, and $\epsilon_-(d, k)$ and π_- denote the same for an individual dynein, when the cargo is in a state $|dk\rangle$. Like forward and backward velocities, the detachment rates also depend on the opposing load per motor:

$$
\epsilon_\pm = \epsilon_\pm^0 f_\pm(\lambda_\pm)
\tag{3}
$$

where the functions $f_\pm(\lambda)$ specify the dependence of the detachment rates on the load per motor $\lambda_\pm$ (given by Eq.2), and $\epsilon_\pm^0$ are the *intrinsic* detachment rate of each

motor, in the absence of any opposing load (by construction, we then require $f_{\pm}(0) = 1$). The precise nature of the function $f_{+}(\lambda)$ has been determined in optical trap experiments for kinesin[23]. It is seen that the dissociation rate (and hence f_{+}) increases rapidly (almost linearly) with load, slowing down close to the stall load ($\approx$ 5pN). For modeling purposes, it is commonly assumed (based on Kramer's rate theory) that $f_{\pm}(\lambda)$ depends exponentially on λ, i.e.,

$$f_{\pm}(\lambda) = \exp\left(\frac{\lambda}{f_{\pm}^{d}}\right), \tag{4}$$

where the parameters $f_{\pm}^{d}$ are specific to each type of motors, and are called *detachment forces*. We will see later that this exponential form in Eq.4, though widely used in modeling studies[8, 9, 10, 24, 25], turns out to be unsuccessful in reproducing the observed bidirectional motion of Dictyostelium endosomes.

We performed Monte Carlo simulations of bidirectional transport using the above model as follows. The cargo with a certain fixed number of attached motors (in the range $D = 1 - 15$ and $K = 1 - 3$) started motion in a certain initial state, which was usually $|10\rangle$. Individual motors are free to attach to and detach from the filament with the rates as mentioned above, thus facilitating changes in the state of the cargo. The cargo moves in the plus direction with a speed v_{+} in $|0k\rangle$ states, where $k > 0$, and in the minus direction with speed v_{-} in the $|d0\rangle$ states, where $d > 0$. All $|dk\rangle$ states with $d > 0, k > 0$ represent TOW situations in which the cargo velocity is small in comparison $v_{\pm}$ (Some typical values are $v_{c}(1,1) = 0.235\mu\text{ms}^{-1}$, $v_{c}(2,1)$=97.07nm s^{-1}, $v_{c}(3,1)$=44.65nm s^{-1} etc.). Such a TOW situation ends when one set of motors give up under the opposing load from the other set. The cargo detaches completely from the filament the moment it assumes the $|00\rangle$ state.

A few simulations were also performed with only similar motors (eg. $K = 0$), so as to reproduce the stalling of a bead coated with a definite number n of dyneins (or kinesins) in an optical trap. In this case, we assume that an opposing load F acts on the bead, whose effect is reflected in the enhanced detachment rate of the motors. The next section discusses how the various single molecule parameters to be used in the simulations were extracted from *vitro* experimental data reported in [3].

3.1. Analysis of in vitro data and extraction of single molecule parameters

In this section, we describe the procedure by which single molecule parameters such as the intrinsic dissociation rates $\epsilon_{\pm}^{0}$, binding rates $\pi_{\pm}$ and detachment forces $f_{\pm}^{d}$ (listed in Table 3) were extracted from the analysis of *in vitro* experimental data reported in Soppina et. al.[3].

It is useful here to introduce the notion of mean first passage time (FPT) $T_{\pm}^{n}(F)$ of an assembly of similar motors, attached to a cargo, which is simply the mean time taken for such a cargo to completely detach from the filament, assuming that the starting state is $|n\rangle$, and an external opposing load F acts on the cargo throughout this time. In optical trap experiments, F is the force exerted by the trap on the bead, while in

Molecular motor	Intrinsic unbinding rate ($\epsilon_\pm^0$)	Binding rate ($\pi_\pm$)	Detachment force $f_\pm^d$
Dynein (-)	$0.667\ s^{-1}$	$2.740\ s^{-1}$	0.546pN
Kinesin(+)	$0.314\ s^{-1}$	$0.904\ s^{-1}$	5.169pN

Table 3. List of single molecule parameters extracted from *in vitro* experiments

in vivo experiments, this force is produced by opposing motors. The general expression for this quantity was derived by Klumpp and Lipowsky[10] (and also in [9]), which we use in the following analysis.

Let us consider the no-load situations first, and put $F = 0$. In this case, the FPT is most easily obtained from the mean run-lengths $\ell_\pm^n$ measured experimentally. Since cargo velocities $v_\pm$ do not significantly depend on motor numbers, these quantities are related as

$$T_\pm^n(0) = \frac{\ell_\pm^n}{v_\pm} \tag{5}$$

For one motor, $T_\pm^1(0) = 1/\epsilon_\pm^0$, therefore, the measured run-lengths immediately give the intrinsic single molecule detachment rates under no load. We now consider a cargo moved by a two-motor assembly. The FPT in this case has the general form (as derived in [10])

$$T_\pm^2(F) = \frac{1}{\epsilon_\pm(F)} + \frac{1}{\epsilon_\pm(F/2)} + \frac{\pi_\pm - \epsilon_\pm(F)}{2\epsilon_\pm(F)\ \epsilon_\pm(F/2)} \tag{6}$$

Putting $F = 0$, we may therefore use the FPT above to deduce the binding rates $\pi_\pm$, after using the experimentally measured two-motor run lengths in Eq.5 to obtain $T_\pm^2(0)$.

Let us now consider the case $F > 0$. In [3], the stall time for beads coated with 1,2 and 3 dyneins (and also 1 and 2 kinesins) were measured directly (reproduced in Table 1). For $n = 1$, the stall time therefore directly gives $\epsilon_\pm(F_\pm^s)$, where $F_\pm^s$ is the stall force for each species. By directly substituting into Eq.3 and Eq.4, we may obtain the detachment forces $f_\pm^d$.

The results of the analysis of this section are summarized in Table 3.

3.2. Load-dependent detachment rate

In the course of a TOW between a single, strong kinesin and several weak dyneins, it is quite likely that there will be many intermediate dynein detachment events. When less than 5 dyneins hold onto the filament, against an opposing load of a kinesin, the individual dyneins (under equal load-sharing assumption) are forced to a situation with super-stall loads. Therefore, a quantitative understanding of the TOW events requires knowledge of the detachment rate of dynein under super-stall load conditions. Although

direct experimental evidence is available now[7, 26]. it is useful to obtain insights into this issue by considering the stall time of multiple motor coated beads under a load equaling the combined stall force of all the motors[3]. For the two-motor case, the experimentally determined stall time is 0.4 seconds. However, when the FPT for this system is computed from Eq.6 using the exponential detachment rate in Eq.4, the result turns out to be ~ 0.133 seconds, which is even less than the one-motor stall time (0.2s).

The reason for the above discrepancy is not hard to understand. Let us first assume that the binding rate of dynein is small (in comparison with its detachment rate). Given that a single dynein will detach within 0.2 s under its stall load, one dynein in a team of two will detach (on an average) in half as much time, i.e, 0.1 s (since the effective detachment rate doubles), which puts the still attached dynein under a load equal to twice its stall force. Therefore, if we apply the rate in Eq.4, the second dynein will detach within a time much less than 0.2 s, consistent with the result obtained here. In order for this not to happen, the binding rate will have to be sufficiently high so that the detached first dynein will manage to rebind before the second dynein also detaches. However, the binding rate thus obtained from Eq.6 turned out to be too high $(102.52 s^{-1})$, in comparison with the value estimated in the previous section from run-length measurements.

A second, and related possibility is that there may be other, non-filament-bound motors coated on the bead at any given point of time. In this case, when one of the bound motors unbinds, the bead may possibly tilt from its original position (relative to the filament), allowing one of the other motors to bind[27]. In this case, therefore, we are dealing with a situation where we have a total of n motors on the bead, but only two can possibly bind to the filament at any point of time (if this were not the case, we would have observed a stalled two-motor bead moving away from the trap center sometimes, which was never seen). However, in order to reproduce the observed stall times, again, the individual binding rate of each motor would have to be too high (eg. $\pi_- \simeq 50$ s^{-1}, 33 s^{-1} and 25 s^{-1} for $n = 3, 4$ and 5 respectively).

We, therefore, considered the possibility that the second dynein, under super-stall load, may not detach as fast as predicted by Eq.4. As the simplest conjecture, we recalculated the FPT using a detachment rate that increases exponentially with load up to the stall force, but saturates at the stall-force level for super-stall loads (motivated partly by experimental data for kinesin [23]), i.e.,

$$f_-(\lambda) = \exp\left(\frac{\lambda}{f_-^d}\right) \qquad \lambda \le F_-^s$$

$$f_-(\lambda) = \exp\left(\frac{F_-^s}{f_-^d}\right) \qquad \lambda > F_-^s \tag{7}$$

With this form for the detachment rate of dynein, and the binding rate in Table 1, the FPT for the two-dynein coated plastic bead under a load $F = 2F_-^s$ turned out to be ~ 0.353s, which is much closer to the experimental value.
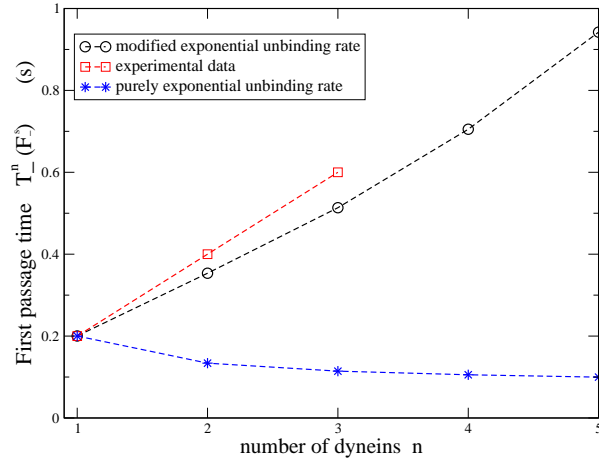
Figure 1. Experimental stall time data(squares, red) of dyneins [3] and FPT with saturating exponential (ref. Eq.7)unbinding rate(black circle) are plotted as a function of number of dyneins. FPT with purely exponential (Eq.4) load dependence(stars, blue) shows clear mismatch with the the experimental data.

Only a few experiments have directly measured detachment rate of dynein at super-stall loads. In [26], it was reported that a single dynein survives only about 0.94 s under a load of 2pN. This does not agree with Eq.7 above (which predicts 0.2s for survival time), while it seems consistent with Eq.4 which predicts 38ms. More recent experiments reported in [7] shows a marked decrease of detachment rate with load in the super-stall regime, in contrast to the sub-stall regime where it increases with load. The detachment rate in Eq.7 is broadly consistent with the data in [7], except for the peak near the stall force. It is also important to note that the abrupt change in the detachment rate at stall load as suggested by Eq.7 need not be taken literally; a smoother change between sub and super-stall loads (eg., tanh function replacing exponential in Eq.4) also produces similar results.

To compute the FPT for beads with 3 and 4 motors attached, we resorted to numerical simulations. The FPT was computed as explained in the last section, and the results are plotted in Fig.1. For comparison, we have also shown the corresponding results with the exponential load-dependent detachment rate. It is clear that the *saturating exponential* form of detachment rate in Eq.7 agrees much better with observations, in comparison with the purely exponential form in Eq.4.

What about the detachment of kinesins at super-stall loads? It is reported in [3] that a single kinesin can sustain a super-stall load of 7.8 pN for about 0.7 seconds. Using the intrinsic detachment rate, binding rate and detachment force for kinesin extracted from experiments (Table 3), the exponential rate in Eq.4 gives a detachment rate of almost exactly 0.7 s, which indeed matches with the experimental value! It appears likely, therefore, that for kinesin, the form in Eq.4 may be appropriate at least for loads less than 7.8pN. Although the behaviour at much larger loads is unknown, and since 5-6 dyneins are enough to stall a kinesin in TOW, we assumed an exponential detachment
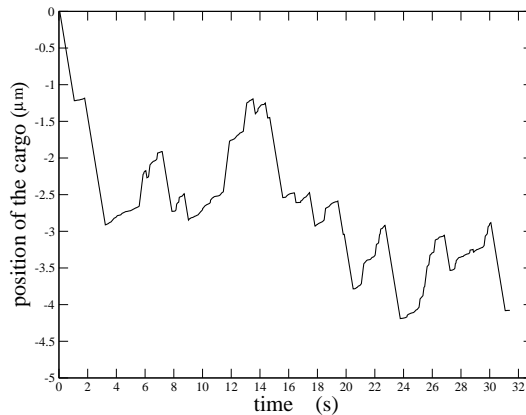
Figure 2. A representative trajectory of cargo pulled by 1 kinesin against 5 dyneins. Trajectory shows frequent TOW phases, and long negative runs, similar to that reported in [3].

rate for kinesin, i.e.,

$$f_+(\lambda) = \exp\left(\frac{\lambda}{f_+^d}\right). \tag{8}$$

Eq.7 and Eq.8 will be used in our simulations described in the next section.

3.3. Numerical simulations of bidirectional transport of endosomes

Having established the mathematical forms for the functions $f_\pm(\lambda)$ to agree with *in vitro* stall time data, we now proceed to model the situation where a set of kinesins and dyneins pull a cargo in opposite directions.

We now used the parameters listed in Table 3 and the detachment rates in Eq.7 and Eq.8 to simulate the motion of an endosome. A single run was continued until the cargo detached from the filament, and various characteristics of the motion (duration of plus/minus runs, duration of TOW events, statistics of reversals etc.) were recorded. For each set of values (D, K), a total of 5×10^5 independent runs of the cargo were used to compute averages.

A typical trajectory of a cargo being pulled by five dyneins against one kinesin is shown in Fig.2. As observed in experiments, frequent pauses in the course of motion are seen, indicating TOW situations. The mean duration of the TOW was found to be in the range 0.43, 0.52 and 0.62 second for one kinesin against 5, 6 and 7 dyneins respectively. These numbers are somewhat smaller, but comparable to the experimental value of ~ 1 second (Table 2). TOW durations for cargo dragged by 2 kinesins against 10 dyneins and 3 kinesins against 9 and 10 dyneins are similar to what was reported recently in human adenovirus transport(2-3 sec), and the total number of motors involved also agrees with the optimal number estimated in these experiments ($\sim$14) [4]. After an
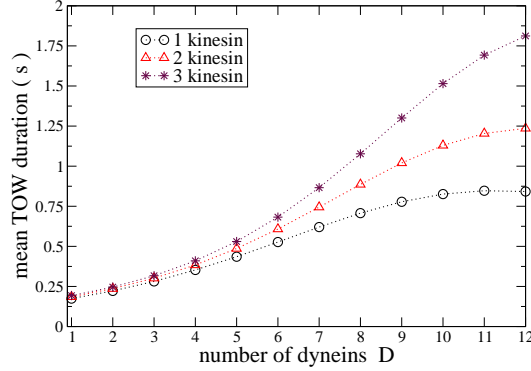
Figure 3. The mean TOW duration increases as we increase dynein numbers, until the point where the kinesin(s) detach under the load of opposing dyneins. In this curve, we have used Eq.7 for the detachment rate of dynein, while the exponential form in Eq.8 is used for kinesin.

initial gradual increase with increasing dynein number, the TOW duration(for fixed number of kinesins) appears to saturate to a value which depends on the number of opposing kinesins, as depicted in Fig.3.

The trajectories observed in simulations also show long negative runs and short positive runs as in the experiments. However, the time-scales here are vastly different: whereas the experimentally observed mean duration of uninterrupted minus-directed and plus-directed runs are nearly 10 s and 5 s respectively (Table 2), the corresponding numbers in the simulations were 1.099s and 0.075s (i.e., for 1 kinesin against 5 dyneins, see Table 4). However, in the experiments, only those TOW events were reported which produced a change of direction of motion of the cargo; short-lived TOW events which failed to produce a reversal in direction were not reported. In order to accommodate this possibility, we carried out a coarse-graining of the trajectories where all pause events which did not result in a change of direction were not counted, i.e., these events were simply absorbed into the runs, which are now called *trips*([2]), to distinguish them from the runs. With this procedure, the mean minus trip time changed very little from the corresponding run time, eg., from 1.099 s to 1.302s for 5 dyneins, but the plus trips were significantly longer than the runs, with the mean time increasing almost four-fold, to 0.307s (Table 5). However, these numbers still significantly fall short of the experimental values. This issue is discussed in more detail in the last section.

Direction reversals: From the simulations, we determined the fraction of TOW/pause events that culminates in a change of direction, separately for TOW events that were preceded by a minus directed run and a plus directed run. In Fig.5, this
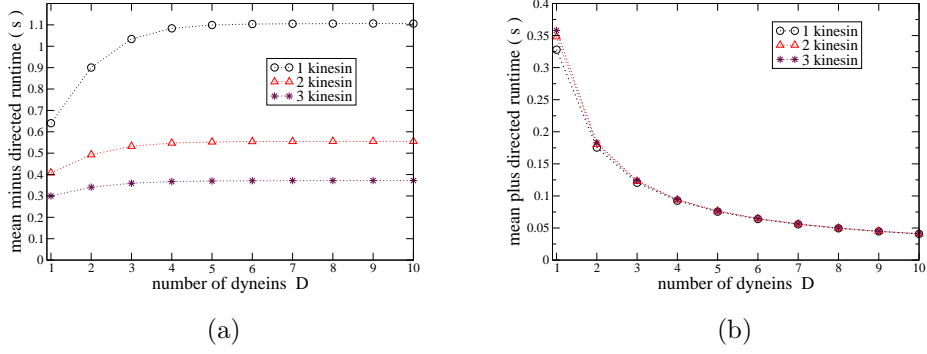
(a) (b)

Figure 4. The mean run-length in the minus(a) and plus(b) direction for varying numbers of kinesin and dynein.

Kinesin	Dynein	distance covered (μm)	TOW(s)	minus run(s)	plus run(s)
	4	-6.84	0.35	1.083	0.092
	5	-14.36	0.43	1.099	0.075
1	6	-26.44	0.52	1.103	0.064
	7	-46.08	0.62	1.105	0.055
	7	-12.10	0.74	0.554	0.056
	8	-25.26	0.88	0.555	0.049
2	9	-47.06	1.02	0.555	0.044
	10	-83.83	1.12	0.555	0.040

Table 4. A summary of results from numerical simulations of endosome transport. The load-dependent detachment rates are taken from Eq.7 and Eq.8

Kinesin	Dynein	distance (μm)	TOW (s)	minus trip (s)	plus trip (s)
	5	-14.36	0.51	1.302	0.307
1	6	-26.44	0.61	1.393	0.304
	7	-46.08	0.71	1.493	0.293
	7	-12.10	0.89	0.908	0.467
	8	-25.26	1.06	1.039	0.471
2	9	-47.06	1.22	1.186	0.452
	10	-83.83	1.37	1.332	0.411

Table 5. The table shows 'coarse-grained' results of numerical simulations, where TOW situations without direction reversals are absorbed into the preceding run. In this table, TOW only refers to those events which are accompanied by direction reversals, and runs are extended to trips (see [2]).
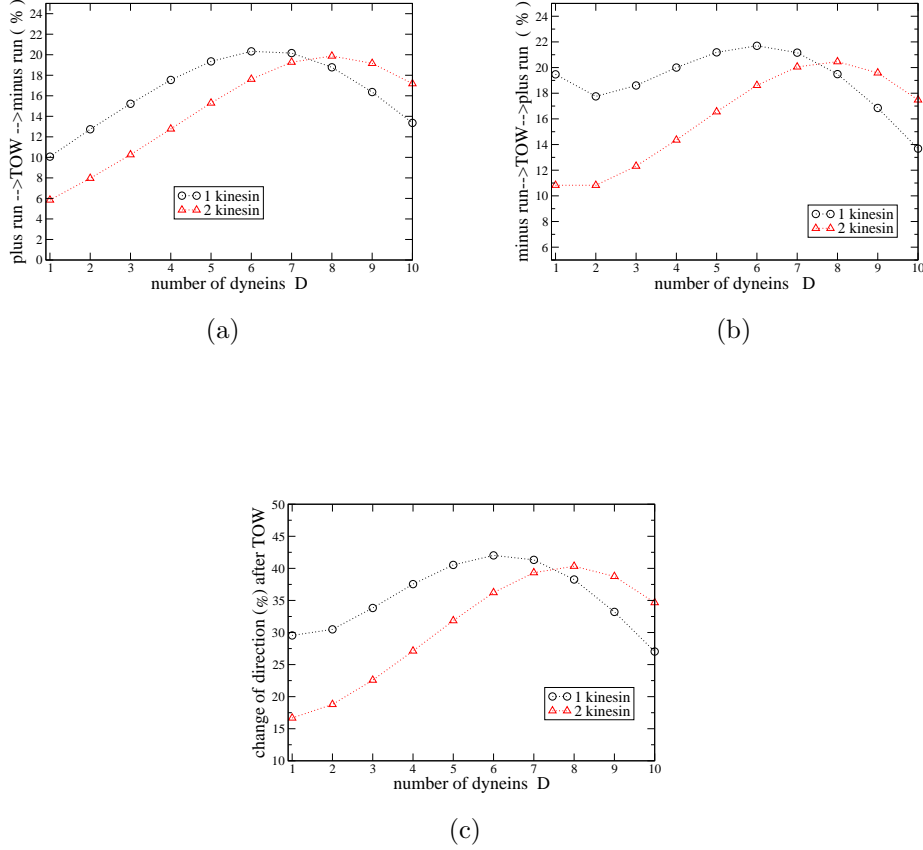
(a)

(b)

(c)

Figure 5. The figure shows the fraction of TOW events that resulted in a reversal in direction, when the TOW was preceded by (a)plus run (b) minus run and (c) either. The data in (c) is therefore simply the sum of that in (a) and (b).

fraction is plotted as a function of the number of dyneins, for a fixed number of opposing kinesins ($K = 1$ or 2), for TOWs following a plus run (Fig.5a), minus run (Fig.5b) and the sum(Fig.5c) of the two separately. Interestingly, we observe that a cargo moving in the plus direction is more likely to continue moving in the same direction after a TOW event, and the same holds true for minus directed runs also. Therefore, the bidirectional cargo motion as a whole, with interspersed plus and minus run segments, may be viewed as a *persistent random walk*.

For $K = 1$, a maximum fraction of reversals (42.02%, see Fig.5c) irrespective of the direction of the initial runs, is observed at $D = 6$ whereas for $K = 2$, the maximum shifts to $D = 8$. The maximization of reversals is likely to be a strategy to effectively "slow down" the cargo so as to increase the number of TOW events before detachment, and therefore the probability of fission. It is interesting that the optimal combination (6 dyneins for 1 kinesin) is close to the experimentally determined ratio from optical trap studies[3] (5-6 dyneins against a kinesin).

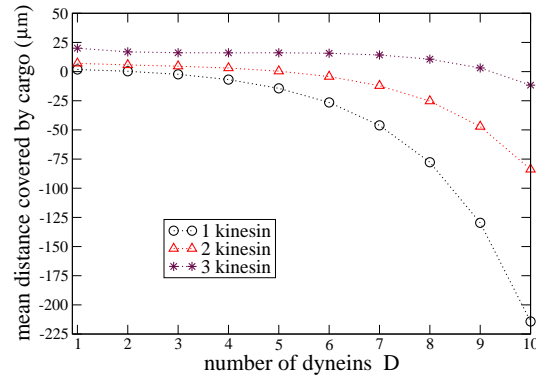*Total distance covered before detachment*: We also determined the mean total

Figure 6. The figure shows the mean total distance moved by the cargo before its eventual detachment from the filament. With the present parameters, 5-6 dyneins are required (against 1 kinesin) to move the cargo over a distance of $\sim 20\mu$m in the minus direction.

distance traveled by a cargo before its eventual detachment from the filament (re-bindings of the cargo to the filament were not considered). In Fig.6, we plot the mean displacement of the endosome from its initial position as a function of the number of dyneins D, for fixed number of kinesins K. For $K = 1$, the mean displacement is positive for $D = 1$ and 2, whereas it is always in the minus direction for $D > 2$. The displacement becomes appreciable (more than 10μm) only for $D > 4$. For large D, the net displacement appears to increase exponentially with D.

What if dynein detachment rate was exponential for all loads? Fig.7 shows the mean TOW duration in this scenario, for varying number of motors. The TOW lasts typically only less than a hundredth of a second in this case! Furthermore, the net transport is seen to be in the plus direction for up to 15 dyneins against a kinesin. Neither of these results agree with experimental observations, which effectively rules out the purely exponential unbinding rate.

4. Discussion

Multiple-motor driven bidirectional transport of cellular cargoes is now established as a widespread phenomenon across a variety of cells. In this paper, we have carried out a numerical simulation study of a model of endosome transport in *Dictyostelium* amoeba reported in [3], in which oppositely pulling dyneins and kinesins engage in a TOW which results in bidirectional transport and occasional fission of the endosome. Our objective was to see how well the observed kinetic features of the bidirectional transport are consistent with (a) single-molecule parameters (binding/unbinding rates) that characterize these motors measured *in vitro* (b) measurements of stall-time of
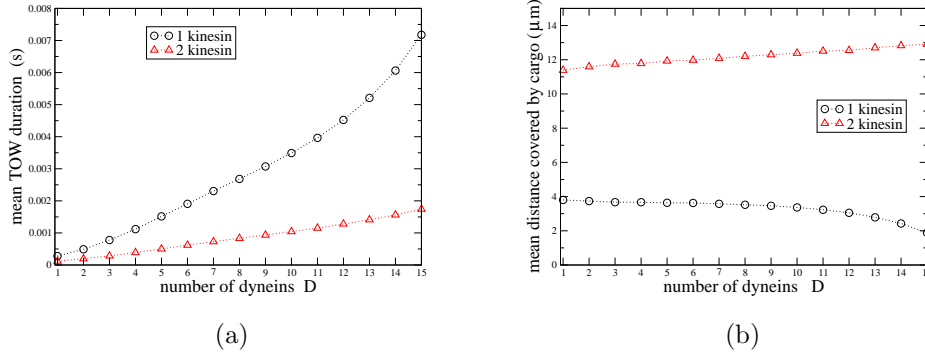
(a)

(b)

Figure 7. Purely exponential load dependence (used for both dynein and kinesin) of unbinding rate shows mismatch with the experimental results. (a) TOW duration is much less than what is observed in experiments (Table 2). (b)The mean net displacement of the cargo is generally positive here, while endosomes in the cell are biased to move in the minus direction on an average.
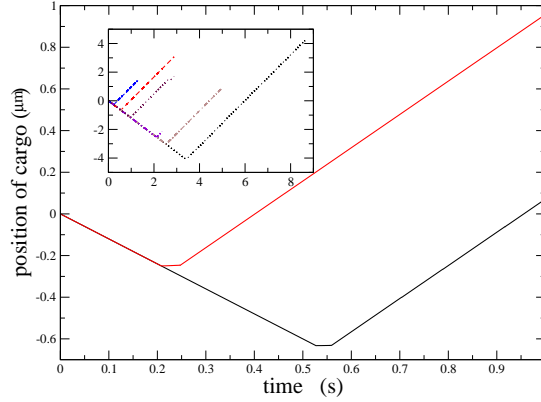

Figure 8. Trajectories of endosomes driven by one kinesin and five dyneins, using the purely exponential form of the detachment rate in Eq.4 for both dyneins and kinesin. Plus run to minus direction reversals can be seen rarely(lass than 0.03%) while minus to plus reversals(2.27%) are much less than what is seen in Fig.5.

individual motors and motor teams in optical traps, and (c) the commonly assumed exponential dependence of detachment rate of a motor on the opposing load.

Our analysis, supplemented with explicit numerical simulations show that the mean duration of the TOW events is consistent with experimental data, provided we assume a somewhat modified form for the load-dependence of the effective single molecule detachment rate of dynein. Essentially, this requires that the detachment rate saturates at super-stall loads, while it increases with load at sub-stall loads. The loss of sensitivity at super-stall loads helps the dynein team to hold their ground against a stronger kinesin

$\pi_-(s^{-1})$	TOW duration (s)		T_- (s)		T_+ (s)	
	before coarse-graining	after coarse-graining	run duration	trip duration	run duration	trip duration
0.005	0.175	0.175	1.069	1.076	2.931	2.941
0.2	0.198	0.217	1.637	1.653	0.764	0.884
0.4	0.216	0.250	2.134	2.161	0.435	0.578
0.6	0.233	0.279	2.524	2.563	0.306	0.462
0.8	0.251	0.305	2.810	2.863	0.236	0.403
1.0	0.269	0.330	3.012	3.080	0.192	0.368
2.0	0.364	0.444	3.400	3.544	0.101	0.314
3.0	0.466	0.550	3.476	3.704	0.069	0.306

Table 6. The table shows results of simulations with a reduced value of $\pi_+ = 0.285s^{-1}$, corresponding to a two-motor run length of $l_+ = 10\mu m$, and π_- varied in the range shown. The results for runs and trips are shown separately. Interestingly, increasing π_- increases T_-, but at the same time, reducing T_+, so an optimal value could not be identified.

in a TOW situation, where the competition is frequently unfair as far as balance of forces is concerned. The dependence of detachment rate on load suggested in this paper is similar to what was found in recent direct optical trap measurements[7].

The principal weakness of the present model is its apparent failure to reproduce simultaneously all the observed features of endosome transport in a consistent manner. In particular, we see a clear mismatch between the binding rates deduced from observed in vitro run lengths (with similar motors) and the termination rates of unidirectional runs between TOW events during bidirectional motion. Some of the possible reasons for this discrepancy are discussed below, within the framework of our model.

(i) It is likely that crowding of motors on the endosome prevents transiently unbound motors from rebinding to the filament at their natural rate, so that unidirectional runs continue longer than they normally should. Indeed, a recent computational study[27] lends some support to this argument. In order to verify how robust the tug of war duration is, against changes in the binding rates of the motors, we carried out simulations with reduced values of both π_+ and π_-, while keeping the intrinsic dissociation rates the same. Reducing π_+ to $0.285s^{-1}$ significantly increased the minus run duration without affecting TOW; however, a similar reduction in π_- reduced the TOW duration *and* the minus run intervals, while extending the plus runs (see Table 6). While the effect of π_- on TOW and plus runs is obvious, the effect on minus run duration is a non-trivial feature. No single set of values of (π_+, π_-) was found to reproduce the experimental numbers for all the three important quantities, i.e., plus run/trip, minus run/trip and TOW duration (data not shown), so this could well be a limitation of the model itself.

(ii) There is a likelihood that motors may detach from and re-attach to the cargo many times within the time scale of observation of transport. In this scenario, during a minus run, frequently, a kinesin may not be present on the cargo at all, and the run is interrupted only when a kinesin first binds to the cargo from solution which then binds to the filament. Therefore, the duration of the plus(minus) run is determined by the (presumably smaller) rate of binding of the dynein(kinesin) to the cargo from cytoplasm. In principle, therefore, this could result in a minus run being extended well beyond the time-scale determined by the binding rate of kinesin. However, it is unclear how this will affect plus runs, as the number of dyneins on the cargo is typically much larger than one.

(iii) Finally, the possibility that a coordinating complex may indeed be responsible for regulating the duration of the runs while active TOW dictates reversals cannot be completely ruled out either.

Among the three possibilities discussed above, we have ruled out (i) after extensive simulations, while a systematic exploration of (ii) will require significant extension of the present model with additional data, well beyond the scope of the present paper. In our opinion, (iii) should be considered seriously after exhausting the other options. At this time, we feel that more experiments on bidirectional transport with detailed measurements of run lengths, pause/TOW events and reversal statistics would be desirable for a better quantitative understanding and characterization of this intriguing phenomenon. In addition, an extension of the present mean-field model to include the motor-motor and motor-cargo interactions[6, 20, 21, 22] could also provide additional insights.

To summarize, we believe that our modeling efforts have yielded important insights into the mechanisms of bidirectional transport driven by TOW between asymmetric motor teams. The highlight of the present paper is the deduction of the non-monotonic nature of the detachment rate of dynein as a function of opposing load, from stall-time measurements done it *in vitro*. We find it interesting and reassuring that the modified detachment rate proposed fits well with *in vitro* stall-time data with beads in optical traps, as well as with tug-of-war data from endosomes. In light of the recent *in vitro* experimental results with dynein from *Drosophila*[7], our studies suggest that this might a universal property of cytoplasmic dynein.

What could be the underlying mechanism for the non-Kramers form of the detachment rate? Recently, Driver et. al. [28] have suggested that load-dependent transport behaviour of multiple-motor teams can be understood better using models which explicitly include intermediate states between the bound and free states, and the transitions between these. Perhaps, a consideration of such intermediate states could provide a clue to the saturation of the dynein detachment rate beyond stall force.

From a statistical perspective, the bidirectional motion of cargoes carried by motors of opposing polarity is a biased random walk, but with a strong history-dependence. The origin of this history-dependence (in the present model) lies in the effective interaction

between opposing motors via load-sharing. We have provided a glimpse of the novel features that arise from this interaction in Fig.5 which shows that the probability of direction reversal following a TOW depends on the direction of the preceding run. A more systematic and extensive investigation of the statistical properties of bidirectional cargo motion with varying motor numbers is presently under progress and will be reported elsewhere.

Acknowledgments

References

[1] Gross S P 2004 Hither and yon: a review of bi-directional microtubule-based transport *Phys. Biol.* **1** R1-R11

[2] Welte M A 2004 Bidirectional Transport along Microtubules *Curr. Biol.* **14** R525-537

[3] V. Soppina *et al* 2009 Tug of war between dissimilar teams of microtubule motors regulates transport and fission of endosomes *Proc. Natl. Acad. Sci. USA* **106**(46) 19381-86

[4] Gazzola M et. al. 2009 A Stochastic Model for Microtubule Motors Describes the In Vivo Cytoplasmic Transport of Human Adenovirus *PLOS Comp. Biol.* **5**(12) e1000623

[5] Shubeita G T *et al* 2008 Consequences of motor copy number on the intracellular transport of kinesin-1 lipid droplets *Cell* **135** 1098-1107

[6] Kunwar A *et al* 2008 Stepping, strain gating, and an unexpected force-velocity curve for multiple-motor-based transport *Curr. Biol.* **18**(16) 1173-83

[7] Kunwar A *et al* 2011 Mechanical stochastic tug-of-war models cannot explain bidirectional lipid-droplet transport *Proc. Natl. Acad. Sci. USA* **108**(47) 18960-65

[8] Müller M J I, Klumpp S and Lipowsky R 2008 Tug-of-war as a cooperative mechanism for bidirectional cargo transport by molecular motors *Proc. Natl. Acad. Sci. USA* **105**(12) 4609-14

[9] Müller M J I, Klumpp S and Lipowsky R 2010 Bidirectional Transport by Molecular Motors: Enhanced Processivity and Response to External Forces *Biophys. J.* **98** 2610-18

[10] Klumpp S and Lipowsky R 2005 Cooperative cargo transport by several molecular motors *Proc. Natl. Acad. Sci. USA* **102** (48) 17284-9

[11] Nascimento A A, Roland, J T and Gelfand V I 2003 Pigment cells: a model for the study of organelle transport *Annu. Rev. Cell Dev. Biol.* **19** 469-91

[12] Gross S P, Welte M A, Block S M and Wieschaus E F 2002 Coordination of opposite-polarity microtubule motors *J. Cell Biol.* **156** 715-24

[13] Valetti C *et al* 1999 Role of dynactin in endocytic traffic: effects of dynamitin overexpression and colocalization with CLIP-170 *Mol. Biol. Cell* **10** 4107-20

[14] Murray J W, Bananis E and Wolkoff A W 2000 Reconstitution of ATP-dependent movement of endocytic vesicles along microtubules in vitro: an oscillatory bidirectional process *Mol. Biol. Cell* **11** 419-33

[15] Smith G A, Gross S P and Enquist L W 2001 Herpes viruses use bi-directional fast-axonal transport to spread in sensory neurons *Proc. Natl. Acad. Sci. USA* **98** 3466-70

[16] Suomalainen M *et al* 1999 Microtubule-dependent plus- and minus end-directed motilities are competing processes for nuclear targeting of adenovirus *J. Cell Biol.* **144** 657-72

[17] McDonald D *et al* 2002 Visualization of the intracellular behaviour of HIV in living cells *J. Cell Biol.* **159** 441-52

[18] Gennerich A and Schild D 2006 Finite-particle tracking reveals submicroscopic-size changes of mitochondria during transport in mitral cell dendrites *Phys. Biol.* **3** 45-53

[19] Arpita Upadhyaya and Michael P. Sheetz 2004 Tension in Tubulovesicular Networks of Golgi and Endoplasmic Reticulum Membranes *Biophysical Journal* **86**(5) 2923-28

[20] Kunwar A and Mogilner A 2010 Robust transport by multiple motors with nonlinear force-velocity relations and stochastic load sharing *Phys. Biol.* **7** 016012

[21] Bouzat S and Falo F 2010 The influence of direct motor-motor interaction in models for cargo transport by a single team of motors *Phys. Biol.* **7** 046009

[22] Bouzat S and Falo F 2011 Tug of war of molecular motors: the effects of uneven load sharing *Phys. Biol.* **8** 066010

[23] Coppin C M *et al* 1997 The load dependence of kinesin's mechanical cycle *Proc. Natl. Acad. Sci. USA* **94** 8539-8544

[24] Grill S W, Kruse K and Jülicher F 2005 Theory of mitotic spindle oscillations *Phys. Rev. Lett.* **94** 108104

[25] Zhang Y and Fisher M E 2010 Dynamics of the tug of war model for cellular transport *Phys. Rev. E* **82** 011923

[26] R. J. McKenney *et al* 2010 LIS1 and NudE Induce a Persistent Dynein Force-Producing State *Cell* **141** 304-314

[27] Erickson R P *et al* 2011 How molecular motors are arranged on a cargo is important for vesicular transport *PLOS Comp. Biol.* **7**(5) e1002032

[28] J.W. Driver *et al* 2011 Productive Cooperation among Processive Motors Depends Inversely on Their Mechanochemical Efficiency *Biophys. J.* **101** 386-395